International Journal of Information, Control and Computer Sciences
ISSN: 2517-9942
Vol:8, No:7, 2014

Design of Regular Communication Area for Infrared Electronic-Toll-Collection Systems

Wern-Yarng Shieh, Chao Qian, Bingnan Pei

Abstract—A design of communication area for infrared electronic-toll-collection systems to provide an extended communication interval in the vehicle traveling direction and regular boundary between contiguous traffic lanes is proposed. By utilizing two typical low-cost commercial infrared LEDs with different half-intensity angles $\Phi_{1/2} = 22^\circ$ and 10°, the radiation pattern of the emitter is designed to properly adjust the spatial distribution of the signal power. The aforementioned purpose can be achieved with an LED array in a three-piece structure with appropriate mounting angles. With this emitter, the influence of the mounting parameters, including the mounting height and mounting angles of the on-board unit and road-side unit, on the system performance in terms of the received signal strength and communication area are investigated. The results reveal that, for our emitter proposed in this paper, the ideal "long-and-narrow" characteristic of the communication area is very little affected by these mounting parameters. An optimum mounting configuration is also suggested.

Keywords—Dedicated short-range communication (DSRC), electronic toll collection (ETC), infrared communication, intelligent transportation system (ITS), multilane free flow.

I. Introduction

FOR electronic-toll-collection (ETC) systems with several down-link and up-link dialogues, or the data transmission between an infrastructure and vehicles through ETC systems, a sufficient communication time interval is necessary to allow for complete transfer of all the information between a roadside unit (RSU) and an on-board unit (OBU) while the vehicles are traveling rapidly through the communication area. In single-lane systems, the vehicle passing through the communication area of an ETC plaza always keeps in the same lane as shown in Fig. 1 (a). However, in multilane-free-flow systems, the vehicle may change travel lanes during data transmission between its OBU and the RSU. As a consequence, the data transmission may be incomplete and has to be performed consecutively by the RSU mounted on the contiguous lane, into which the vehicle has just entered (see Fig. 1 (b)). Hence, it is necessary to decide the timing to separate the data transmission into segments for corresponding traffic lanes while the vehicles change lanes [1]. For this purpose, a regular boundary of the communication area between contiguous traffic lanes is beneficial as shown in Fig. 1 (b) by the three dashed rectangles. On the contrary, for conventional ellipse-like communication regions it is not very easy to decide the timing to separate the data transmission as the rightmost dashed ellipse in Fig. 1 (b) shows.

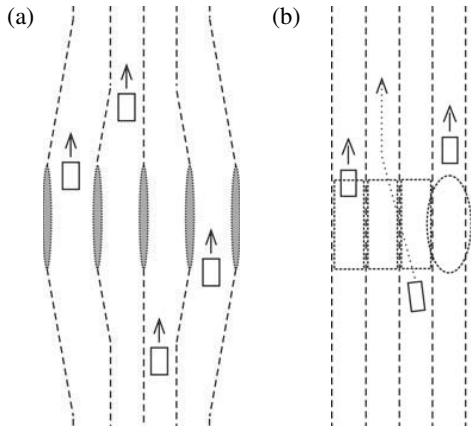

Fig. 1. Scenario of electronic-toll-collection plaza of (a) single-lane and (b) multilane-free-flow systems. The three dashed rectangles and the dashed ellipse in (b) illustrate the communication area of each traffic lane.

Infrared short-range communication systems in the wave-length band 780-950 nm are suitable for ETC applications due to their low cost and simple technology. In this wavelength range, low-cost light-emitting diodes (LED) and p-i-n photodiodes are commonly used for the source of the transmitter and the detector of the receiver, respectively. For ETC applications, there is an effective physical model proposed not long ago to estimate the performance of the system in terms of the received signal strength and communication area [2]. The communication area can be effectively tailored by a proper design of the radiation pattern of the emitter [3]–[7]. In this paper we present a successful design of an infrared emitter to achieve regular boundaries of the communication areas between contiguous traffic lanes, and the regular characteristics of the communication boundary are very little affected by the mounting parameters of the system.

II. Signal-Strength Relation

In ETC systems there are two data-transmission paths: up-link and down-link. They can be treated with the same physical model. Because in general the signal power of down-link is much stronger than that of up-link, therefore whether the up-link data transmission is successful determines

W.-Y. Shieh is with the Department of Electronic Engineering, St. John's University, Tamsui District, New Taipei City, Taiwan 25135. (e-mail: shiehwy@mail.sju.edu.tw).

C. Qian and B.-N. Pei are with the Department of Information Engineering, Dalian University, 116622, China. (e-mail: 56581101@qq.com, bnpei@ieee.org).

This is a cooperative work between St. John's University and Dalian University. The corresponding author is Bingnan Pei.

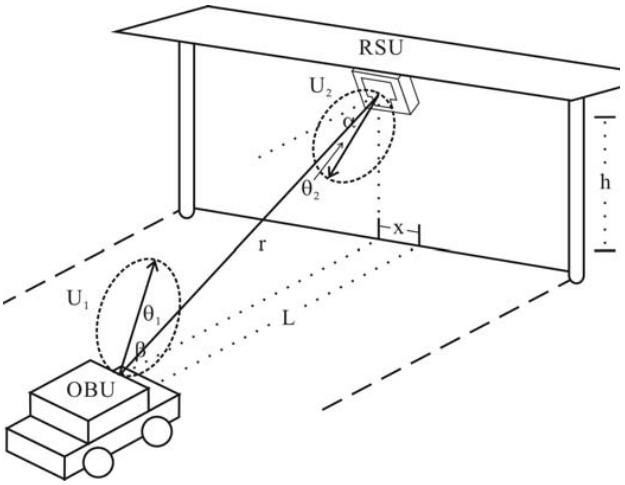

Fig. 2. Typical mounting configuration of ETC systems.

whether the whole data transmission is complete. Thus in this paper we focus only on the up-link data transmission, the calculation of down-link transmission may follow in a similar manner.

A. Signal-Strength Physical Model

Fig. 2 shows a typical scenario for ETC systems, where α is the RSU declining angle, β is the OBU upward-inclining angle, and h is the vertical mounting height of the RSU relative to the horizontal plane of the OBU. An OBU (vehicle) travels through the communication area with a lateral distance x relative to the vertical plane (yz plane) above the central line of the traffic lane. To facilitate the discussion, we set the coordinates of the RSU as (0, 0, h), and the OBU (vehicle) traveling in the y-direction on the xy plane has the coordinates (x, L, 0), where L is the longitudinal distance of the OBU relative to the vertical plane (xz plane) of the RSU.

The physical model for infrared short-range communication systems utilizing light-emitting diodes (LEDs) and p-i-n photodiodes as emitting and receiving components, respectively, has been established in our previous works for electronic toll collection (ETC) [2]–[7] and intervehicle communication [8]. The signal strength received by the receiver and emitted by the emitter can be described by

$$S = A_0 \frac{U_1(\theta_1, \phi_1)\, U_2(\theta_2, \phi_2)}{r^2}, \tag{1}$$

where A_0 is the amplitude constant, $U_1(\theta_1, \phi_1)$ is the radiation pattern of the emitter, $U_2(\theta_2, \phi_2)$ is the receiving pattern of the receiver, and r is the distance between the emitter and the receiver. U_1 and U_2 are functions of emitting direction (θ_1, ϕ_1) and receiving direction (θ_2, ϕ_2), respectively, where θ_1, ϕ_1, and θ_2, ϕ_2 are defined following the conventional spherical polar coordinates relative to the normal of the corresponding module, i.e., the emitter and the receiver.

For infrared communication systems, p-i-n photodiodes are very often used as the signal detector. In our systems, we utilized planar p-i-n photodiodes as the receiver whose receiving pattern can be described with high precision by a simple cosine function, i.e., $\cos\psi$, where ψ is the incident angle of the signal relative to the normal of the diode facet. This means that for our physical model in (1), the receiving pattern of the receiver can be described by

$$U_2(\theta_2, \phi_2) = \cos\theta_2 \tag{2}$$

with high precision. Interested readers can refer to the sketch of this pattern in our previous work (see Fig. 3 in [2]).

For an OBU emitter composed of several different LEDs, each has a different half-intensity angle $\Phi_{1/2}$ and with a different mounting angle relative to the normal of the OBU, (1) can be described by

$$S_n = \frac{1000}{9} \frac{\left[\sum_{i=1}^{m} A_i \cos^{n_i}\theta_{1i}\right] \cos\theta_2}{r^2}, \tag{3}$$

where m is the number of LEDs consisting the emitter, θ_{1i} is the angle between the data transmission line (line r in Fig. 2) and the normal direction (symmetric axis) of the LED, and θ_2 is the angle between the data transmission line and the normal direction of the RSU (receiver). In this equation, A_i and n_i are related by conservation of energy which has been shown to be [9]

$$A_i = \frac{(n_i + 1)\, P_i}{2\pi}, \tag{4}$$

where P_i is the radiant power of the corresponding LED, and n_i can be obtained from its half-intensity angle $\Phi_{1/2}$ by

$$n_i = -\frac{\ln 2}{\ln\cos\Phi_{1/2}}. \tag{5}$$

In addition, the constant 1000/9 in (3) was decided by a technique called *arbitrary scale* [2], which leads to the result that when $S_n > 1$, the data transmission can be successful; otherwise it fails. The arbitrary-scale technique is performed with the aid of a measurement of the available communication length of the system under a certain configuration. This measured communication length can be used to determine the communication boundary. In the analysis we compare all the received signal strengths with that at the communication boundary, which is normalized to 1. The details of all these discussions can be found in our previous works [2]–[8], especially in [2].

B. Construction of the Emitter

From many low-cost infrared LEDs commercially available, we select two LEDs with half-intensity angle $\Phi_{1/2} = 22^\circ$ and 10°, respectively, to construct the emitter. Typical specifications of such LEDs are available in the manufacturer's datasheets, for example in [10] and [11]. It is assumed that all the LEDs we utilized emit the same total radiant power under the same operating conditions irrespective of their half-intensity angles. This is reasonable for LEDs fabricated with the same manufacturing process but only capsulated in different plastic lenses to form the radiation patterns with different half-intensity angles.

We construct the emitter with 14 LEDs, seven having half-intensity angle $\Phi_{1/2} = 10^\circ$ and the other seven having

TABLE I
MOUNTING ANGLES OF THE LEDS IN THE EMITTER

LED	1	2	3	4	5	6	7	8	9	10	11	12	13	14
$\Phi_{1/2}$	10°	10°	10°	10°	10°	10°	22°	22°	10°	22°	22°	22°	22°	22°
θ'	15°	15°	15°	15°	0°	0°	0°	0°	-16°	-16°	-16°	-16°	-16°	-16°

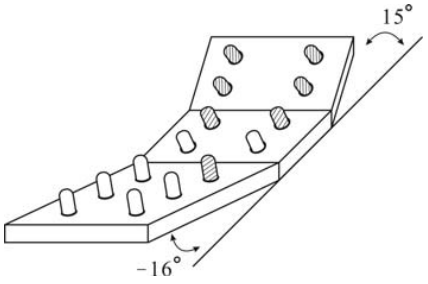

Fig. 3. "Three-piece" emitter with different mounting angles 15°, 0°, and -16°, respectively, in which seven LEDs have half-intensity angle $\Phi_{1/2} = 10^\circ$ (filled with slash lines), and the other seven have half-intensity angle $\Phi_{1/2} = 22^\circ$.

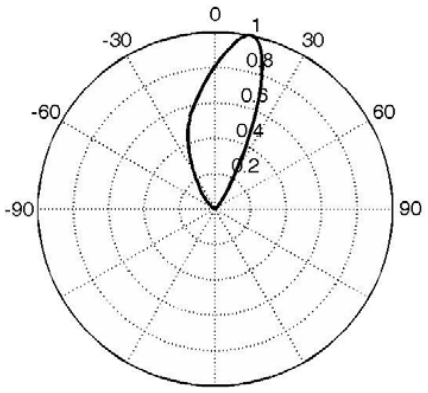

Fig. 4. Radiation pattern of the emitter.

$\Phi_{1/2} = 22^\circ$ in a three-piece structure. Their mounting angles θ' relative to the normal of the emitter along the longitudinal direction, i.e., vehicle traveling direction, are: 15° (four), 0° (four), and -16° (six), respectively, as shown in Fig. 3 and Table I, where the positive value indicates far direction and the negative near direction. The aforementioned mounting angles of the constituent LEDs are obtained with the aid of an optimization algorithm [3]–[6]. The radiation pattern of this emitter along the longitudinal direction with its maximum value normalized to 1 is shown in Fig. 4.

III. RESULTS OF ANALYSIS

Based on (3), by utilizing the aforementioned emitter in the OBU, the normalized signal strength received by the RSU from the OBU emission can be described by

$$S_n = \frac{1000}{9} \frac{\left[\sum_{i=1}^{14} A_i \cos^{n_i}\theta_{1i}\right] \cos\theta_2}{r^2}, \qquad (6)$$

where n_i can be obtained easily from (5) as $n_i = 9$ for $\Phi_{1/2} = 22^\circ$, and $n_i = 45$ for $\Phi_{1/2} = 10^\circ$. In this equation, for the convenience of comparison, the corresponding amplitude constants A_i are further normalized as

$$A_i = \frac{1}{14}$$

for $\Phi_{1/2} = 22^\circ$, and

$$A_i = \frac{4.6}{14}$$

for $\Phi_{1/2} = 10^\circ$, such that the emitter presented here and the other ones which we designed previously in [2]–[7] all have the same total radiant power under the same operating conditions irrespective of the number of LEDs in the emitter.

A. Received Signal Strength, Communication Area, and the Influence of the OBU Mounting Height

Figs. 5 (a), (b), and (c) show the three-dimensional profile of S_n for $\alpha = 45^\circ$, $\beta = 45^\circ$, and $h = 4.0\,\text{m}$, 4.5 m, and 5.0 m, respectively. The difference in vertical height h may correspond to OBUs mounted on different kind of vehicles such as small cars, vans, trucks, $\cdots$ etc. Because S_n is symmetric to the y-axis, in these figures we sketch only the part for which $x > 0$. Figs. 6 (a), (b), and (c) show the corresponding contours of S_n. In these figures the contours indicated by 1, 2, 3, or 4 denote the corresponding values of S_n. From Fig. 5, as expected, we see that the received signal strength drops quickly when the lateral distance x increases. However, the contours keep a "long-and-narrow" shape as shown in Fig. 6. Figs. 5 (a), (b), and (c) show that the received signal strength is stronger for smaller vertical height h due to the relatively shorter distance between the RSU and the OBU. Most importantly, the "long-and-narrow" shape of the received signal-strength contours is not affected by the variation of h as can be seen from Fig. 6. This means that for all kinds of vehicles, i.e., small cars, vans, trucks, $\cdots$ etc., we have regular communication boundaries between contiguous traffic lanes. This is beneficial for both multilane-free-flow and single-lane applications.

B. Influence of the OBU Mounting Angle

Figs. 7 (a) and (b) illustrate the three-dimensional profile of S_n for $h = 5.0\,\text{m}$, $\alpha = 45^\circ$, and $\beta = 30^\circ$, $\beta = 60^\circ$, respectively. Figs. 8 (a) and (b) show the corresponding contours of S_n. These figures are to be compared with Figs. 5 (c) and 6 (c) for the same mounting parameters of $h = 5.0\,\text{m}$ and $\alpha = 45^\circ$, but different β, to help us understand the influence of the OBU up-inclining angle on the received signal strength and the communication area. As can easily be seen by comparison of these figures, the overall received signal strength S_n increases with the increase of β, and the communication area recedes toward the direction of the RSU. This property is a generic characteristic of the

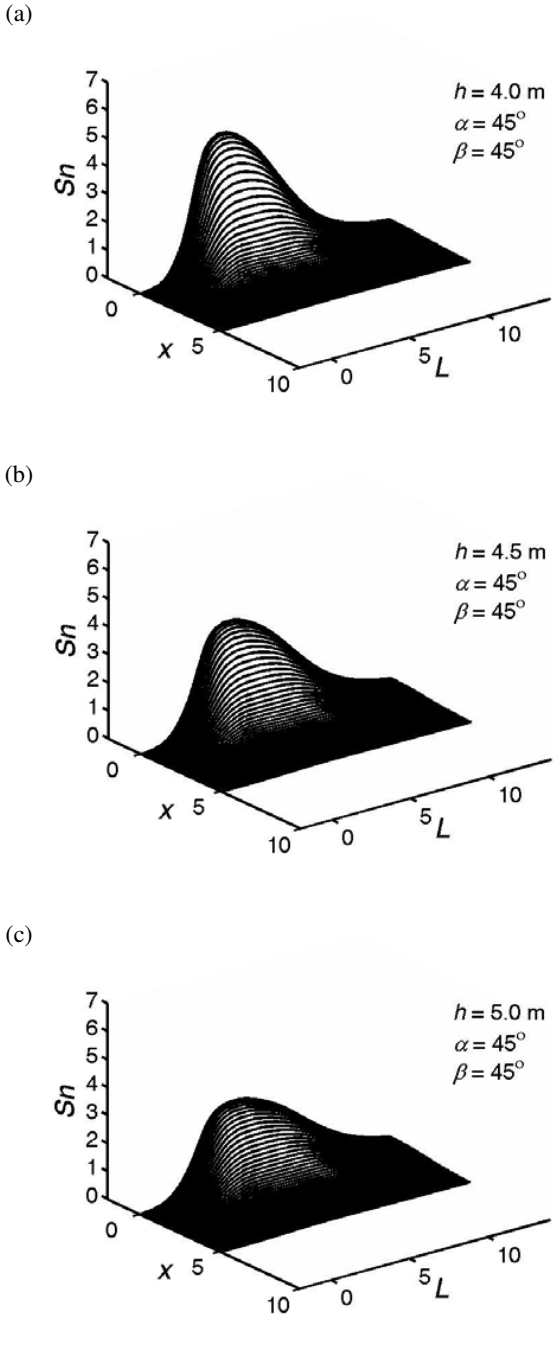

Fig. 5. Three-dimensional plot of the normalized signal strength received by the RSU from the OBU emission for $\alpha = 45°$, $\beta = 45°$, (a) $h = 4.0$ m, (b) $h = 4.5$ m, and (c) $h = 5.0$ m.

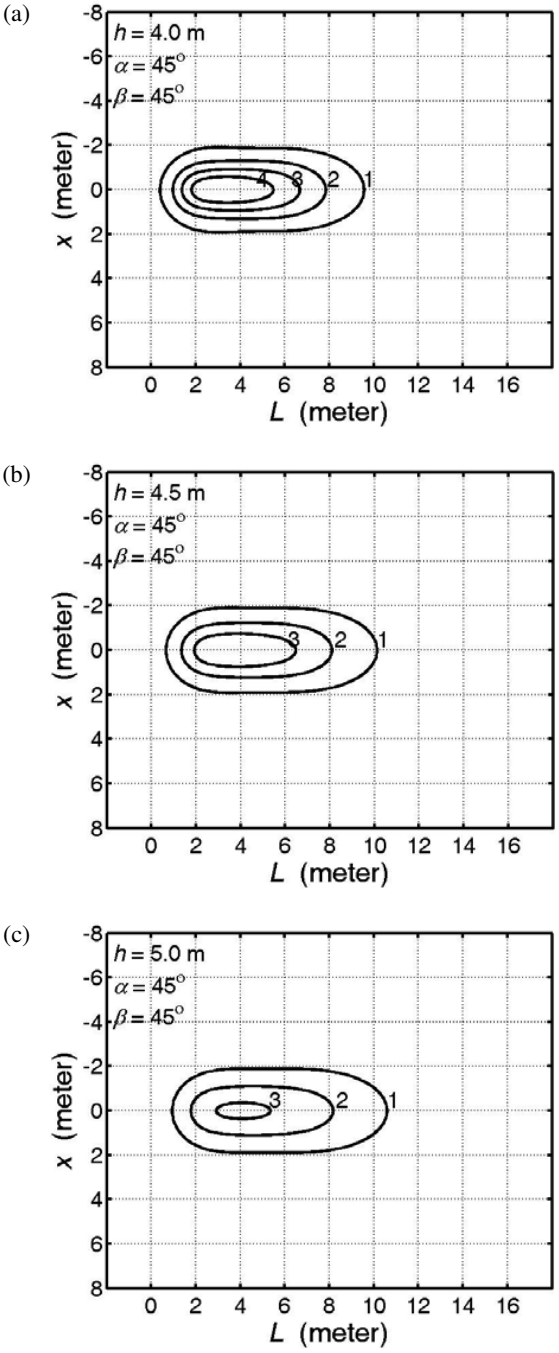

Fig. 6. Contours of the normalized signal strength received by the RSU from the OBU emission for $\alpha = 45°$, $\beta = 45°$, (a) $h = 4.0$ m, (b) $h = 4.5$ m, and (c) $h = 5.0$ m.

mounting angle of the emitter due to its high directivity [2]. Notice that for $45° < \beta < 60°$, the received signal-strength contours can keep "long-and-narrow" shape as revealed by Figs. 6 (c) and 8 (b), and the received signal strength is relatively high as can be seen from Figs. 5 (c) and 7 (b). For $\beta < 45°$, the received signal strength is relatively low, and the "long-and-narrow" characteristic of the signal-strength contours is gradually disrupted. This leads to irregular boundaries of the communication areas between contiguous traffic lanes. When β near $30°$, the condition is very poor as shown in Figs. 7 (a) and 8 (a). Therefore, in order to obtain regular boundaries of the communication area and high signal strength, for the OBU emitter introduced in this paper, it is necessary to keep the OBU up-inclining angle β between $45°$

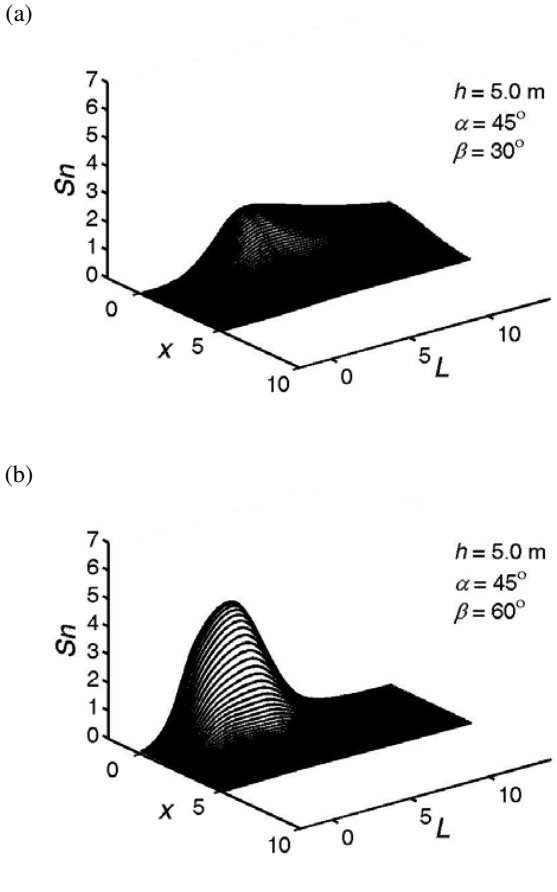

Fig. 7. Three-dimensional plot of the normalized signal strength received by the RSU from the OBU emission for $h = 5.0\,\mathrm{m}$, $\alpha = 45°$, and (a) $\beta = 30°$, (b) $\beta = 60°$.

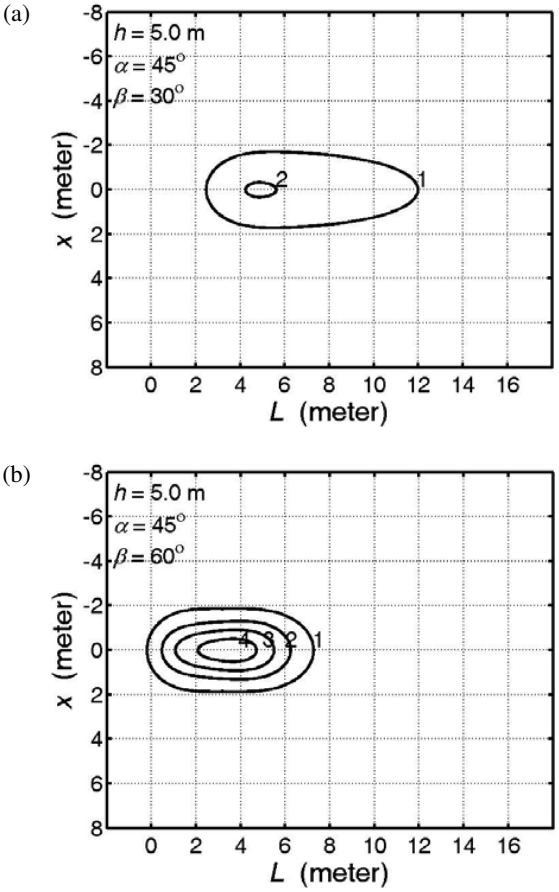

Fig. 8. Contours of the normalized signal strength received by the RSU from the OBU emission for $h = 5.0\,\mathrm{m}$, $\alpha = 45°$, and (a) $\beta = 30°$, (b) $\beta = 60°$.

and $60°$.

C. Influence of the RSU Mounting Angle

Figs. 9 (a) and (b) illustrate the three-dimensional profile of S_n for $h = 5.0\,\mathrm{m}$, $\beta = 45°$, and $\alpha = 30°$, $\alpha = 60°$, respectively, and Figs. 10 (a) and (b) show the corresponding contours of S_n. Similarly to the previous subsection, these figures are to be compared with Figs. 5 (c) and 6 (c), for the same parameters of $h = 5.0\,\mathrm{m}$ and $\beta = 45°$, but different α, to grasp the influence of the RSU declining angle on the received signal strength and the communication area.

As can be seen by comparing aforementioned figures, the effect of the RSU declining angle is similar to that of the OBU up-inclining angle, but the influence is not so high due to the relatively less directivity of the RSU receiver [2]. The overall received signal strength S_n increases slightly with the increase of α, and the communication area recedes a trifle toward the direction of the RSU (comparing Figs. 10 (a), 6 (c), and 10 (b)). For both $\alpha = 30°$ and $\alpha = 60°$, the characteristic of the "long-and-narrow" shape of the received signal-strength contours is affected only slightly.

IV. Conclusions

A "long-and-narrow" communication area between the OBU and the RSU with regular boundaries between contiguous traffic lanes is beneficial for both single-lane and multilane-free-flow ETC systems. To achieve this requirement, we propose a simple three-piece structure to adjust the spatial distribution of signal power by a proper design of the radiation pattern of the emitter. The emitter is composed of two different LEDs with half-intensity angle $\Phi_{1/2} = 22°$ and $10°$, respectively. There are totally 14 LEDs in this three-piece array and the structure is very easy to fabricate. With this emitter utilized in the OBU, the influence of the mounting parameters, including the mounting height of the OBU relative to the RSU, and the mounting angles of the OBU and the RSU, on the system performance in terms of the received signal strength and the communication area are analyzed.

The results show that the "long-and-narrow" shapes of the received signal strength contours are affected very slightly by the mounting height of the OBU and the mounting angle of the RSU. However, the mounting angle β of the emitter, i.e., the OBU, is influential due to the higher directivity of its radiation pattern. For $\beta < 45°$, the received signal strength is relatively low, and the characteristic of the "long-and-narrow" shape of

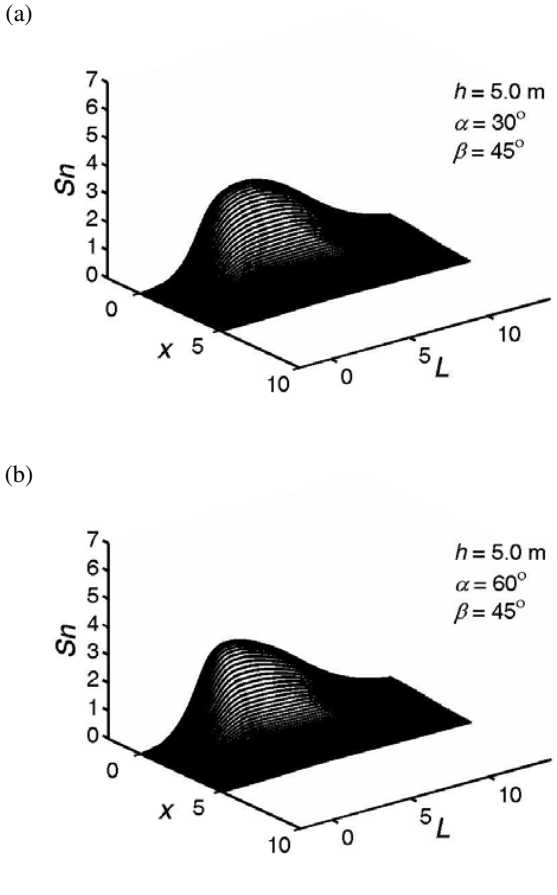

Fig. 9. Three-dimensional plot of the normalized signal strength received by the RSU from the OBU emission for $h = 5.0\,\mathrm{m}$, $\beta = 45°$, and (a) $\alpha = 30°$, (b) $\alpha = 60°$.

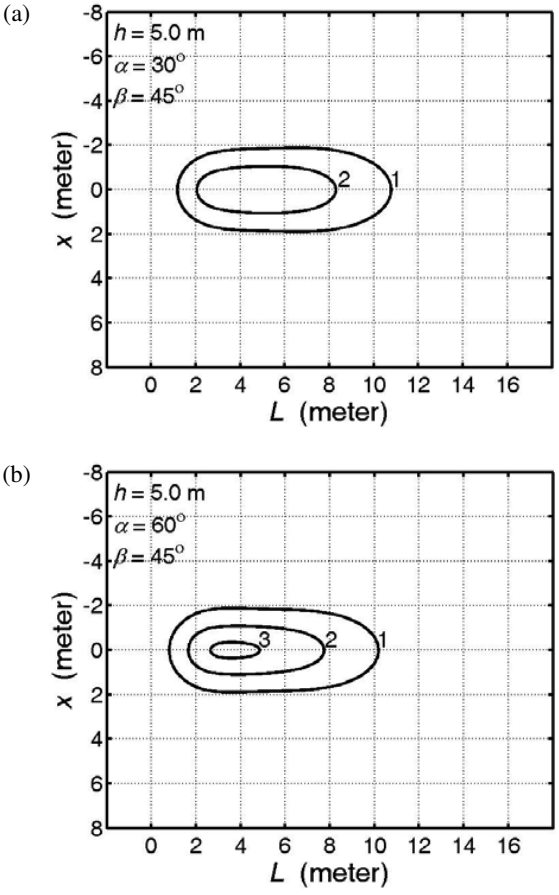

Fig. 10. Contours of the normalized signal strength received by the RSU from the OBU emission for $h = 5.0\,\mathrm{m}$, $\beta = 45°$, and (a) $\alpha = 30°$, (b) $\alpha = 60°$.

the received signal-strength contours is disrupted. This will lead to irregular boundary of the communication area. When β near 30°, the condition is very poor. Therefore, the OBU up-inclining angle of $45° < \beta < 60°$ is recommended.

Acknowledgement

The authors are grateful to the National Center for High-Performance Computing for its support of facilities and software.

References

[1] W.-Y. Shieh, W.-H. Lee, S.-L. Tung, and C.-D. Ho, "A novel architecture for multilane-free-flow electronic-toll-collection systems in the millimeter-wave range", *IEEE Trans. Intell. Transport. Syst.*, vol. 6, pp. 294-301, Sep. 2005.

[2] W.-Y. Shieh, W.-H. Lee, S.-L. Tung, B.-S. Jeng, and C.-H. Liu, "Analysis of the optimum configuration of roadside units and onboard units in dedicated short-range communication systems", *IEEE Trans. Intell. Transport. Syst.*, vol. 7, pp. 565–571, Dec. 2006.

[3] W.-Y. Shieh, T.-H. Wang, Y.-H. Chou, and C.-C. Huang, "Design of the radiation pattern of infrared short-range communication systems for electronic-toll-collection applications", *IEEE Trans. Intell. Transport. Syst.*, vol. 9, pp. 548–558, Sep. 2008.

[4] W.-Y. Shieh, C.-C. Hsu, S.-L. Tung, P.-W. Lu, T.-H. Wang, and S.-L. Chang, "Design of infrared electronic-toll-collection systems with extended communication areas and performance of data transmission", *IEEE Trans. Intell. Transport. Syst.*, vol. 12, pp. 25–35, Mar. 2011.

[5] W.-Y. Shieh, C.-C. Hsu, and T.-H. Wang, "A problem of infrared electronic-toll-collection systems: the irregularity of LED radiation pattern and emitter design", *IEEE Trans. Intell. Transport. Syst.*, vol. 12, pp. 152–163, Mar. 2011.

[6] W.-Y. Shieh, T.-H. Wang, H.-F. Lin, J.-Y. Chang, and C.-H. Lin, "Design of infrared electronic-toll-collection systems with LEDs with irregular radiation pattern", in *Proc. 2011 IEEE Int. Conf. on Veh. Electro. and Safe.*, Beijing, China, July 10–12, 2011, pp. 124–129.

[7] W.-Y. Shieh, H.-C. Chen, and T.-H. Wang, "A method to withstand high signal attenuation for infrared electronic-toll-collection systems—equivalent strength of the received signal in the communication area", in *Proc. 2012 IEEE Int. Conf. on Veh. Electro. and Safe.*, Istanbul, Turkey, July 24–27, 2012, pp.223–227.

[8] W.-Y. Shieh, H.-C. Chen, T.-H. Wang, and B.-W. Chen, "Exploration of the communication area of infrared short-range communication systems for intervehicle communication", *Proc. WASET*, vol. 79, pp. 971–976, July, 2013.

[9] J. M. Kahn and J. R. Barry, "Wireless infrared communications", *Proc. IEEE*, vol. 85, pp. 265-298, Feb. 1997.

[10] *Datasheet of TSFF5400 High Speed Infrared Emitting Diode, 870 nm, GaAlAs Double Hetero*, Mar. 2005. The Vishay website, 81016.pdf. [Online]. Available: http://www.vishay.com/docs/81016/

[11] *Datasheet of TSFF5200 High Speed Infrared Emitting Diode, 870 nm, GaAlAs Double Hetero*, Mar. 2005. The Vishay website, 81060.pdf. [Online]. Available: http://www.vishay.com/docs/81060/